

**SUPPLEMENTARY MATERIAL TO:**

**Origin of oceanic ferrodiorites by injection of nelsonitic melts in gabbros at the Vema  
Lithospheric Section, Mid Atlantic Ridge**

*Daniele Brunelli<sup>1,2</sup>, Alessio Sanfilippo<sup>3</sup>, Enrico Bonatti<sup>2,4</sup>, Sergei Skolotnev<sup>5</sup>, Javier Escartin<sup>6</sup>,  
Marco Ligi<sup>2</sup>, Giorgia Ballabio<sup>1</sup>, Anna Cipriani<sup>1,4</sup>*

*1 - Dipartimento di Scienze Chimiche e Geologiche, Università di Modena e Reggio Emilia, Modena, Italy.*

*2 – Istituto di Scienze Marine, ISMAR-CNR, Bologna, Italy.*

*3 - Dipartimento di Scienze della Terra e dell'Ambiente, Università degli Studi di Pavia, Pavia, Italy.*

*4 - Lamont-Doherty Earth Observatory, Columbia University, NY, USA.*

*5 - Geological Institute, Russian Academy of Sciences, Moscow, 119017 Russia*

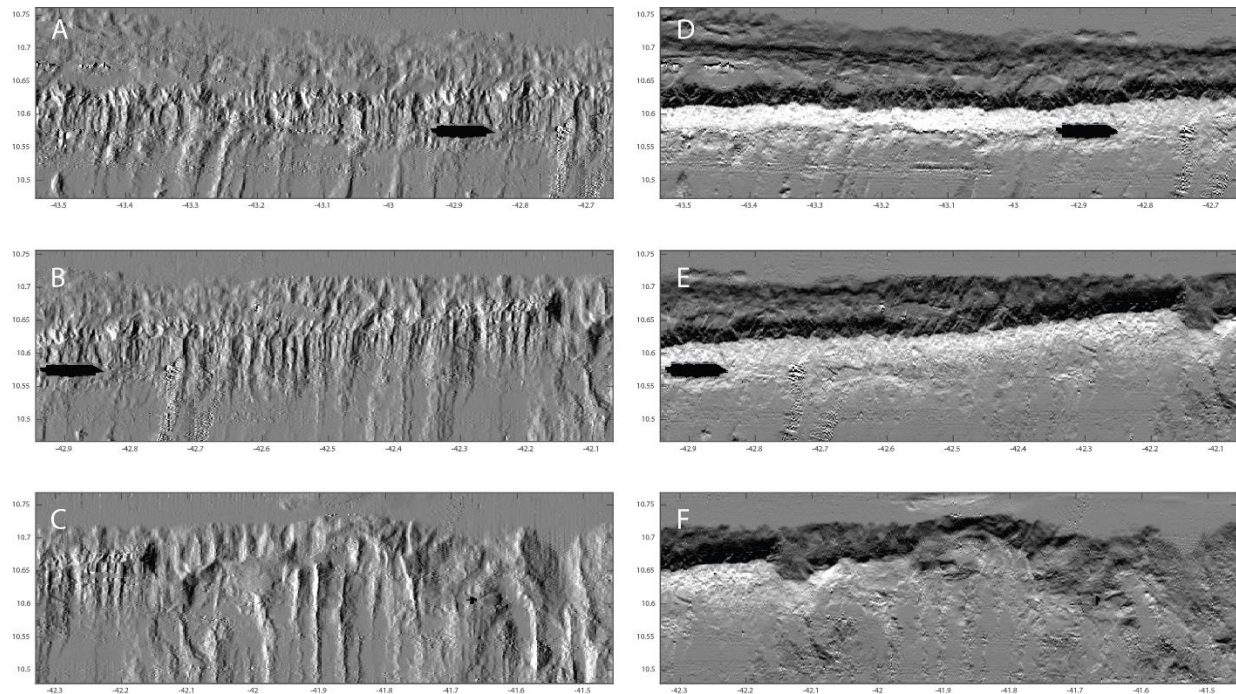
*6 - Laboratoire de Géologie, UMR 8538, Ecole Normale Supérieure, PSL Research University, CNRS, Paris, France*

Supplementary Figure 1                      pag. 2

Supplementary Figure 2                      pag. 3

Supplementary Figure 3                      pag. 4

## SUPPLEMENTARY FIGURE 1



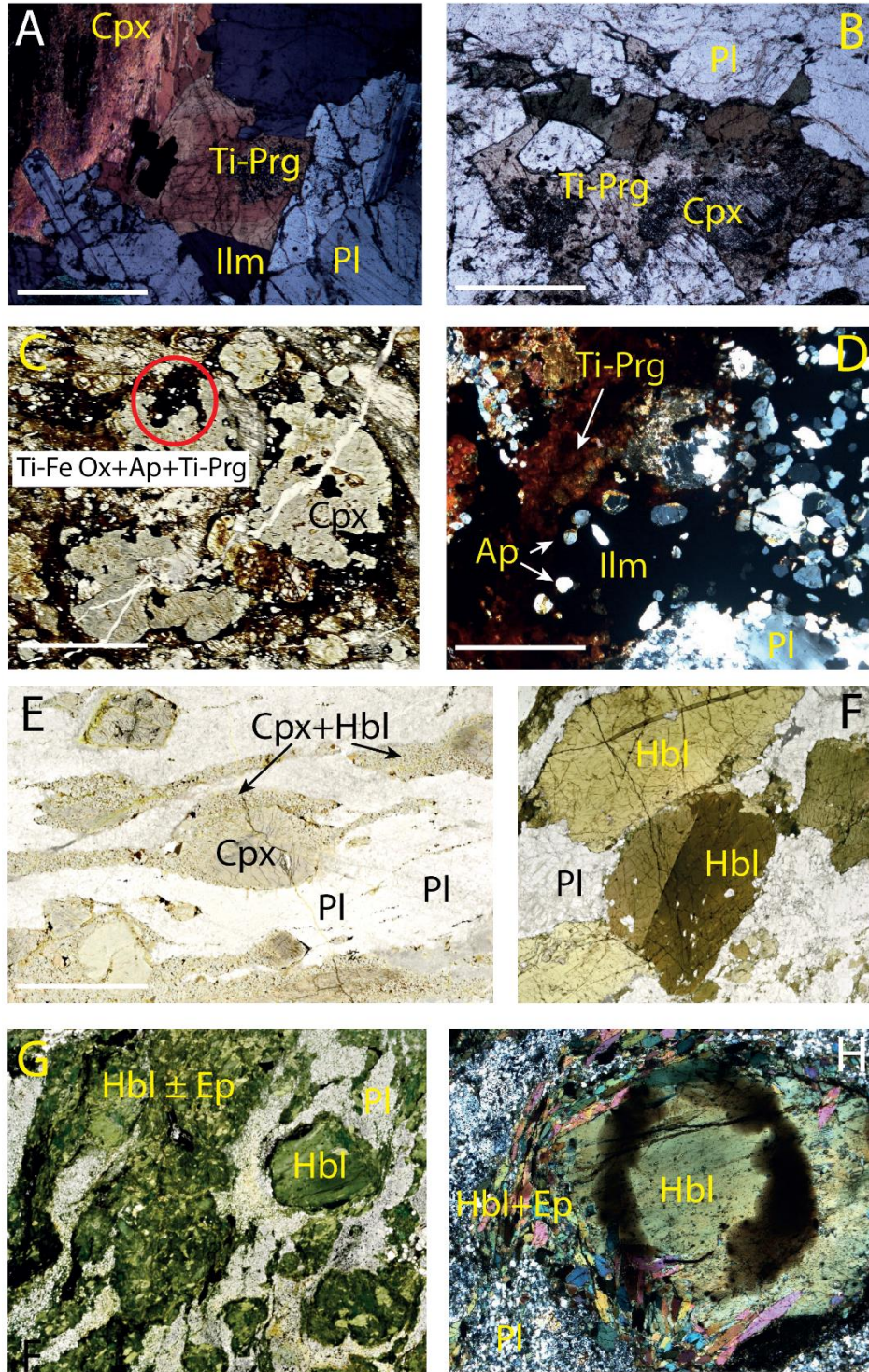
Gradient map of the Vema Transverse Ridge (VTR).

A-C) E-W oriented gradient map enhancing the tectonic relief and slope oriented sub-perpendicular to the transform, and related to the abyssal hill fabric parallel to the axis. From West (A) to the East (B-C) the abyssal hill fabric shows slight variations in spacing. All abyssal hills and associated faults terminate near or at the summit of the VTR.

D-F) Gradient maps in the N-S direction: in this map, as well as in the shaded relief maps (e.g. Fig. 1), no evidence of oceanic detachment faults can be detected. They would be characterized by parallel corrugations in the direction of spreading (sub-parallel to the transform fault).

On this basis, we infer that the 26 Ma of spreading in this area corresponds to oceanic crust formed in a magmatically robust ridge axis with symmetric spreading, precluding the formation of oceanic core complexes associated with asymmetric spreading at low melt supply.

**SUPPLEMENTARY FIGURE 2**





Representative examples of the different textural types of amphiboles described in the text:

(A) and (B): type 1 amphibole (sample L2616-09, scale bar = 0.5 mm): Ti-pargasitic amphibole (Ti-Prg) interstitial to plagioclase (Pl) and clinopyroxene (Cpx) and including ilmenite (Ilm).

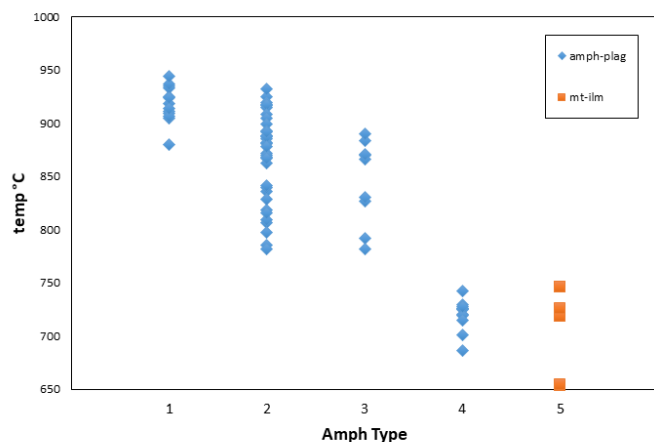
(C): Type 2 amphibole (sample S2221-59). Large porphyroclastic Cpx partly corroded and replaced by an assemblage of Fe-Ti Ox, apatite (Ap) and Ti-Prg (scale bar = 2mm). A detail of this assemblage is shown in (D): Ti-Prg associated to Ap+Ilm and in disrupted fine grained plagioclase matrix (scale bar = 1 mm).

(E): Type 3 amphibole (sample S1925-19). Mylonitic gabbro with Cpx porphyroclasts mantled by a neoblastic assemblage of Cpx+Hbl±Pl (scale bar = 5 mm) in sample L2630-03.

(F): Mildly deformed Hbl porphyroclasts in highly amphibolitized gabbros.

(G-H): Type 4 amphibole (sample S1907-31). Highly amphibolitized gabbros. The original gabbro minerals are completely replaced by pseudomorphs of green hornblende and epidote. Deformation at low metamorphic conditions is attested by the fine-grained assemblage of secondary Hbl+Ep (±Pl±Chl).

### SUPPLEMENTARY FIGURE 3



Estimated Am-Pl (Holland and Blundy, 1994) and Mag-Ilm (Buddington and Lindsley, 1964) equilibration temperatures plotted according to the amphibole petrographic types as described in the text.